Lasers in Manufacturing Conference 2025

Towards velocity-based feedback control in laser cutting: benchmarking system capability on an industrial case study

Sofia Guerra[a,b], Leonardo Caprio[a], Matteo Pacher[c], Davide Gandolfi[c], Mattia Vanin[c], Mara Tanelli[b], Sergio M. Savaresi[b], Barbara Previtali[a]

[a]*Department of Mechanical Engineering, Politecnico di Milano, Via La Masa 1, 20156 Milano (MI), Italy*
[b]*Department of Electronics, Information and Bioengineering, Politecnico di Milano, via G. Ponzio 34/5, 20133 Milano (MI), Italy*
[c]*Adige SpA, BLM Group, Via per Barco 11, 38056 Levico Terme (TN), Italy*

Abstract

To meet stringent requirements in terms of productivity and efficiency, the industry is shifting towards machine tools with sensors and auto-tuning capabilities enabled by Artificial Intelligence (AI) algorithms. Accordingly, in laser cutting the coaxial monitoring of the molten pool provides relevant information that can be interpreted by means of Machine Learning (ML) approaches to enable real-time velocity-based feedback control. In the present research, a holistic control architecture was thus developed and validated on an industrial case-study to demonstrate its applicability. Targeting iso-quality conditions, experiments on sample geometries on 5 mm thick stainless steel allowed to showcase an increase in productivity whilst avoiding critical defects such as cut dominated by plasma formation or loss of cut. The results obtained may be extended to a wide range of materials and sheet thicknesses demonstrating the generalized applicability of the technological framework.

Keywords: Laser cutting; Machine learning; Process control

1. Introduction

High-power fusion laser cutting is a well-established technique for processing metal sheets and tubes of millimeter-range thicknesses. In both scientific and industrial communities, there is an ongoing interest in enhancing productivity and maintaining high-quality results. In this context, the application of monitoring sensors to gain insights into the process is highly valuable to sense the cut edge quality. The most employed monitoring techniques are based on photodiodes and camera-based solutions. The first ones were exploited to identify loss of cut or plasma-dominated cutting states (Adelmann et al., 2016; Schleier et al., 2017). On the other hand, there is a strong evidence in the scientific community that camera-based solutions have a stronger potential thanks to the possibility of collecting spatially resolved information. In this case, different camera configurations can be implemented, i.e. off-axis side view or coaxial view (Poprawel & Konig, 2001; Wen et al., 2012). Furthermore, the collected process images can be utilized together with Machine Learning (ML) and Artificial Intelligence (AI) techniques to sense and detect the cut quality. This has been implemented for both the fusion laser cutting (Pacher et al., 2020),(Pacher et al., 2019) and the reactive fusion laser cutting processes (Pacher et al., 2023). Moreover, according to the estimated cut quality, real-time control techniques may be exploited to regulate process parameters, with the goal of increasing the process productivity and improving the final cut quality. In this framework, speed regulation control schemes have been developed and tested in real-time to minimize the dross of the cut edge profile (Guerra et al., 2025; Pacher et al., 2020). However, in an industrial scenario, there are still some open challenges, such as the loss of cut or plasma-dominated state, which can occur at high cutting speed values. Both of these two cutting states should be avoided due to their destructive nature on the final cut quality.

The present work proposes a novel control architecture to improve process productivity whilst maintaining iso-quality conditions. Exploiting a NIR coaxial camera monitoring architecture, a real-time dross attachment estimate and cut class classifier were developed and then employed together to build a supervisor logic and closed-loop control scheme to regulate the cutting speed (Pacher, Gandolfi, et al.). The presented approach was finally tested in real-time on an industrial case-study during the fusion cutting of 5mm thick stainless steel, maximizing productivity and cut quality, whilst preventing the formation of typical cut-quality defects such as plasma and loss of cut. Furthermore, the presented architecture was validated by cutting a real-case demonstrator geometry, highlighting the generalized applicability of the technological framework to industrially relevant case studies.

2. Materials and method

2.1. Experimental setup

An industrial laser cutting machine (LC5, Adige-SYS S.p.A. BLM Group, Levico Terme (TN), Italy) was used to realize the experiments of this work. The employed laser source (YLS-6000-CUT, IPG Photonics) is a 6-kW fiber laser source, with a 100 µm core diameter. Moreover, the collimation and the focalization lens of the cutting head are respectively of 75mm and of 155mm. Furthermore, a CMOS coaxial camera (xiQ MQ013MG-ON, Ximea GmbH, Münster, Germany) was employed to acquire melt pool images. The process emission light is then filtered in the 700-1000 nm wavelength band. The laser cutting system and the coaxial camera monitoring architecture are shown in Fig 1. Furthermore, Table 1 reports the main specifications.

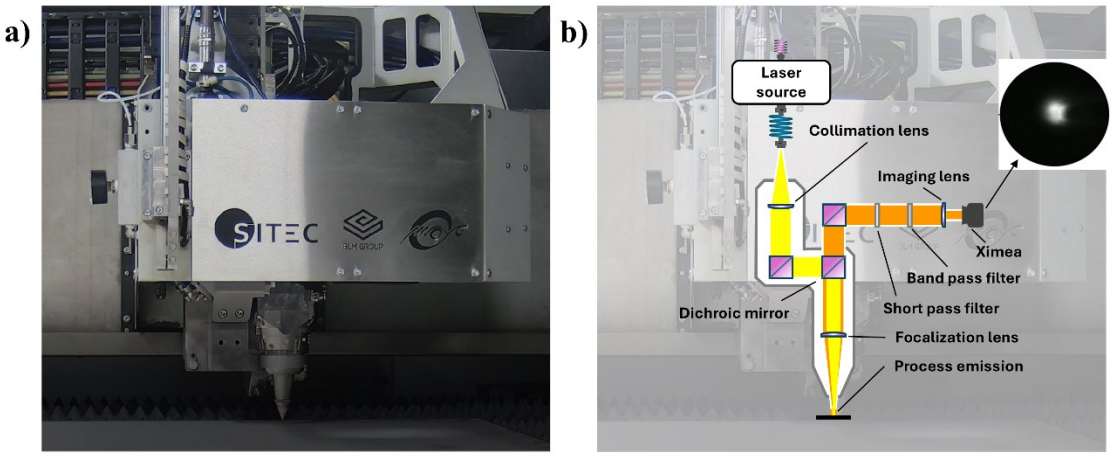

Fig. 1. (a) Laser cutting head and monitoring system; (b) Working scheme of the main components

Table 1. Laser cutting and monitoring system specifications

Laser cutting and monitoring systems	
Parameter	**Value**
Emission wavelength, λ (nm)	1070
Collimation length, f_{col} (mm)	75
Fiber core diameter, d_{core} (µm)	100
Focalization length, f_{foc} (mm)	155
Beam waist diameter, d_0 (µm)	207
Maximum power, $P_{\max}$ (kW)	6
Wavelength observation band, λ_{obs} (nm)	700-1000

The monitoring system allows the acquisition of process emission images of the melt pool, subsequently analysed for the training of the dross attachment estimate and cut class classifier models. Fig 2 shows an example of the images analysis pipeline: firstly, the original frame is binarized applying a hard thresholding at different binarization levels, then a series of geometrical features (i.e. Area, Length, Width, Perimeter, Lag, etc.) is extracted and employed as input of the ML algorithm training phase.

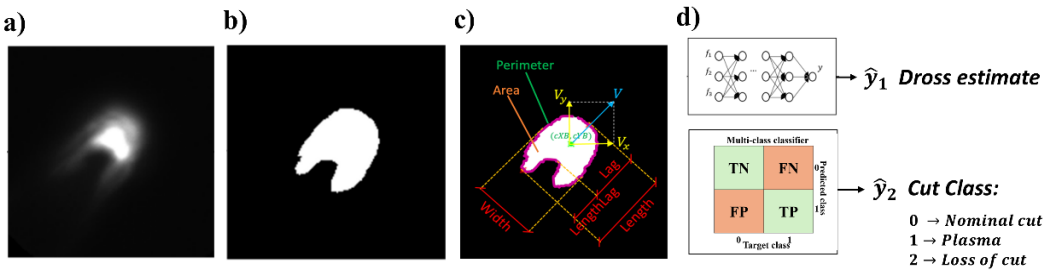

Fig. 2. Image analysis pipeline: (a) original captured frame; (b) hard thresholding of the gray-scale image; (c) extraction of geometrical features; (d) dross estimate and cut class classifier models training

2.2. Experimental design

The scope of this research was to develop a novel control scheme based on the dross estimate and cut class classifier, together with a supervisor control logic, with the goal of improving productivity, by regulating the speed in real-time, maintaining iso-quality conditions. To realize this, the dross attachment estimate proposed previously by (Guerra et al., 2025) was taken as a reference and complemented with the cut class classifier, to correctly detect plasma formation or loss of cut condition. The aim of the experimental design was to induce quality variations on the cut profile in terms of different process states that could occur during the fusion laser cutting.

The employed material was 5 mm thick AISI304 stainless steel. The starting point of the experimental campaign corresponds to optimized process parameters. The laser power was set to 6 kW with a nozzle diameter of 2mm and the N_2 assisting gas pressure was set to 18 bar. Moreover, the focal position of the laser beam was kept Δf = -5.7mm, the stand-off distance at 0.7 mm. The cutting speed was employed as variable parameter to determine different process states in terms of cut quality condition (i.e., standard cut, plasma cut, loss of cut). Moreover, different cutting directions were required and applied during the experimental campaign to develop a robust ML algorithm (Guerra et al., 2025), suitable for an industrial applicability of the approach. Table 2 shows the fixed and variable parameters of the experimental campaign.

Table 2. Fixed and variable parameters of the experimental campaign to train the cut class classifier

Fixed factors	**Value**
Material	AISI304
Thickness (mm)	5
Power, P (W)	6000
Assist gas	N_2
Pressure, p (bar)	18
Nozzle diameter, d_{noz} (mm)	2.0
Stand-off distance, SOD (mm)	0.7
Focus, Δf (mm)	-5.7
Variable factors	**Value**
Cutting speed v (mm/min)	5000-6000-7000-8000
Cutting direction, θ (degree)	0-90-180-270

2.3. Machine Learning approach

Following the dataset acquisition from the experimental campaign of Section 2.2, a supervised Machine Learning approach was exploited to construct a classifier model for the process state condition. The cut samples were labelled after observing the process and assessing the cut profile in terms of process state (cut class “0”, “1”, “2”, respectively for standard cut, plasma cut, loss of cut).

A multiclass random forest algorithm was selected to classify the process state condition in real time. Other ML algorithms were trained and tested but such performances are not reported in this work for conciseness. The experimental design resulted in a full dataset of 232242 points, which have been divided in 70% for the training phase (with 10-fold cross validation) and 30% for the testing phase.

The selected random forest classifier presents equal class weight for the three process state conditions, a max_depth parameter of 7, and 7 estimators.

The performance of the cut class classifier was evaluated based on statistical indicators, such as the Accuracy of the model, the Precision (*P*), the Recall (*R*) and the F1-score, defined as follows:

$$Accuracy = \frac{TP + TN}{Total\ samples} \tag{1}$$

$$P = \frac{TP}{TP + FP} \tag{2}$$

$$R = \frac{TP}{TP + FN} \tag{3}$$

$$F1 = 2 * \frac{P * R}{P + R} \tag{4}$$

where TP, FP, TN and FN stand for True Positive, False Positive, True Negative and False Negative, respectively, and are the outputs of the algorithm’s confusion matrix.

2.4. Closed-loop control architecture based on dross estimate, cut class classifier and switching supervisor

The aim of the presented research is to regulate the cutting speed in real time, maximizing productivity and preventing the formation of typical cut quality defects, such as plasma-dominated state and loss of cut. To realize that, a closed-loop control architecture based on a dross estimate model and cut class classifier was constructed, as schematized in Fig 3.

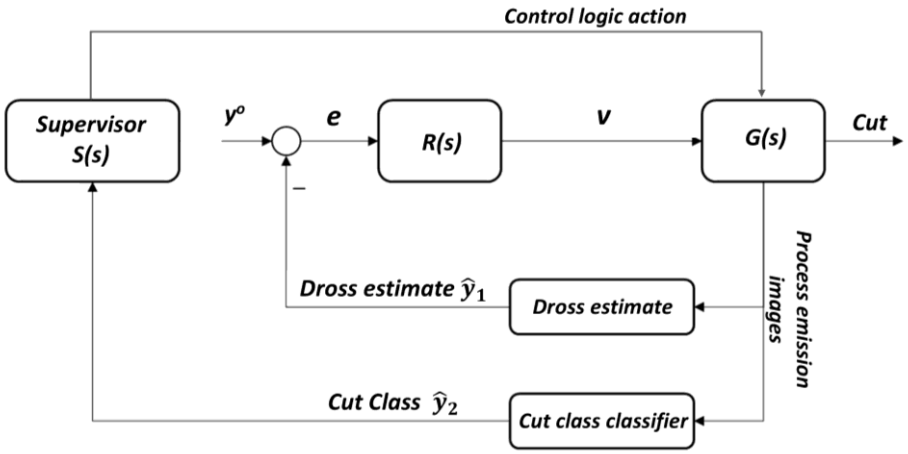

Fig. 3. Schematic representation of the developed closed-loop control architecture

The two mentioned cut quality models were designed exploiting process relevant information extracted from melt pool emission images which have been collected from a NIR coaxial camera monitoring system, as discussed by Mazzoleni (Mazzoleni et al., 2020) . The output provided by the dross attachment estimate ($\hat{y}_1$) is compared with a user defined reference value y^0, and a Proportional-Integral (PI) regulator *R(s)* is employed to regulate the cutting speed in real-time to track it, as discussed and implemented previously. Furthermore, the output of the cut class classification algorithm ($\hat{y}_2$) is then provided to a supervisor logic *S(s)* which developed a control logic action that is superimposed to the updated cutting speed *v* provided by PI regulator. More in particular, if the detected process state is loss of cut or plasma-dominated cut then the speed controller provides a constant decrement of 0.1% of the current set value. On the other side, if the classifier detects a standard process condition, the PI regulator is responsible for the real-time speed control to track the dross reference set-point y^0.

2.5. Experimental design for controller architecture testing

After the development of the control architecture, different real-time control experiments were designed and realized to test the control system in different and industrially relevant conditions. The fixed factors remained consistent with the previous experimental design, while the variable factor was the initial set velocity v_i, which was regulated by the controller. Table 3 presents the fixed and variable parameters of the experimental campaign to test the real-time control system.

Table 3. Fixed and variable parameters of the real-time control system tests.

Fixed factors	**Value**
Material	AISI304
Thickness (mm)	5
Power, P (W)	6000
Assist gas	N_2
Pressure, p (bar)	18
Nozzle diameter, d_{noz} (mm)	2.0
Stand-off distance, SOD (mm)	0.7
Focus, Δf (mm)	-5.7
Variable factors	**Value**
Starting cutting speed v (mm/min)	5200-8000

The first experiment considers the case in which a conservative value of cutting velocity is selected corresponding to the standard value for 5 mm thick stainless steel (i.e. 5200 mm/min). Hence, the controller must be capable of increasing the speed whilst avoiding plasma and loss of cut formation. On the other hand the second control experiment starts from loss of cut condition with an initial cutting speed of 8000 mm/min. Therefore, the controller must activate itself to decrease the cutting velocity and regain standard processing conditions.

Furthermore, in industrial settings, custom geometries often feature segments with varying directions and curvature. To demonstrate the effectiveness of the developed closed-loop control in such environments, the system was tested on a complex shape, i.e. a design object with a vase shape, as shown in Fig 4. The vase geometry was ad-hoc designed by the authors with the different varying segments and curvatures to test and underline the applicability of the presented technological framework and control scheme to industrially relevant case studies.

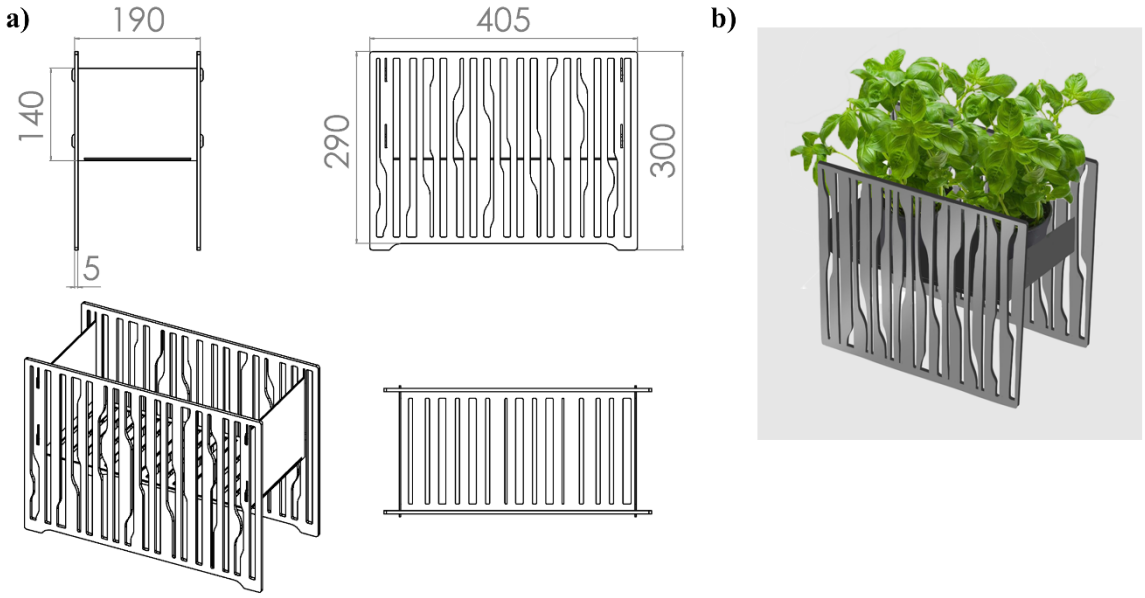

Fig. 4. Design of the demonstrator vase geometry: (a) Technical drawing of the vase geometry with principal dimensions; (b) Expected outcome of the vase demonstrator.

3. Results

3.1. Cut class classifier model

As previously mentioned, the feature selection stage is a crucial step in selecting indicators that are correlated to the investigated cut quality defects (i.e. dross attachment, plasma formation and loss of cut) but at the same time not influenced by the cutting direction. Since the cut class classifier model should work in real-time with the dross attachment estimation algorithm (Guerra et al., 2025), the authors employed the same features selected by the Maximum Relevance Minimum Redundancy (MRMR) algorithm utilized for the Neural Network dross estimation model developed in previous works.

In this section, the results of the supervised classification algorithm are shown in the confusion matrices of Fig 5 (a) for the training phase and Fig 5 (b) for the testing phase. Furthermore, from the confusion matrices results, the previously mentioned statistical indicators were evaluated to characterize the cut class classifier model performances. Table 4 shows the model performances in terms of Accuracy, Precision (P), Recall (R) and F1-score for the investigated cut class quality. It is possible to observe that a high level of model accuracy can be achieved in both the training and testing phase, corresponding to 99.9% and 99.9% respectively.

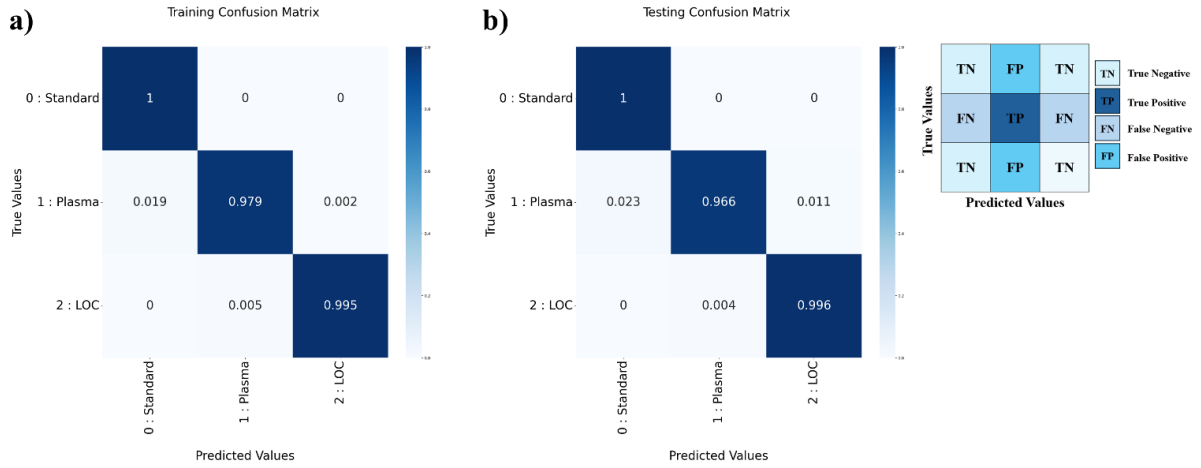

Fig 5. Confusion matrix of the training phase (a) and the testing phase (b) of the selected cut class classifier model.

Table 4. Performances of the cut class classifier model in terms of Accuracy, Precision (*P*), Recall (*R*) and F1-score

Model	Cut Class	Training			Testing		
		P	R	F1	P	R	F1
Random Forest Classifier	0: Standard	99.9%	100%	99.9%	99.9%	100%	99.9%
	1: Plasma	98.3%	97.9%	98.1%	98.6%	96.6%	97.6%
	2: LOC	99.9%	99.5%	99.7%	99.7%	99.6%	99.6%

3.2. Real-time closed loop control of the process

As previously mentioned, to demonstrate the feasibility of the developed approach for control applications, closed-loop real-time control experiments were realized. Fig 6 shows the results for different starting conditions.

In Fig 6 (a) the controller starts from a low level of initial cutting speed (i.e. v_i = 5200 mm/min), which corresponds to a standard cut condition. Due to the difference between the estimated dross (blue signal) and reference (red signal) dross, the control architecture gradually increases the speed up to the final optimal value of v_f = 6240 mm/min (Fig 6 (b)), according to the target dross level set at 0.02 mm. Moreover, it can be observed, from the blue cut class signal of Fig 6 (b), that the process state condition is detected correctly by the cut class classifier (i.e. standard cut), resulting in a cutting speed increase.

In the second experiment the process starts in a loss of cut dominated state from a high initial cutting speed of 8000 mm/min, (shown in blue in Fig 6 (c)) as detected by the classifier (cut class = 2). Therefore, the controller decreases the cutting speed to overcome this critical process condition, transitioning through the plasma-dominated state (cut class = 1) and finally achieving a cutting speed that provides a standard cut condition. As a consequence, the PI controller regulates the speed to the final value of v_f = 5940 mm/min (Fig 6 (d)) to reach the target dross level set at 0.02 mm.

Furthermore, few peaks in the dross estimate signal can be observed in both of the experiments, which correspond to passages of the laser cutting head on the supporting laser grid that influence the image analysis and models training phases, as mentioned by Guerra (Guerra et al., 2024). For this reason, the developed ML models and control architecture were designed to maintain robust performance under the grid disturbance, as realized in the mentioned work.

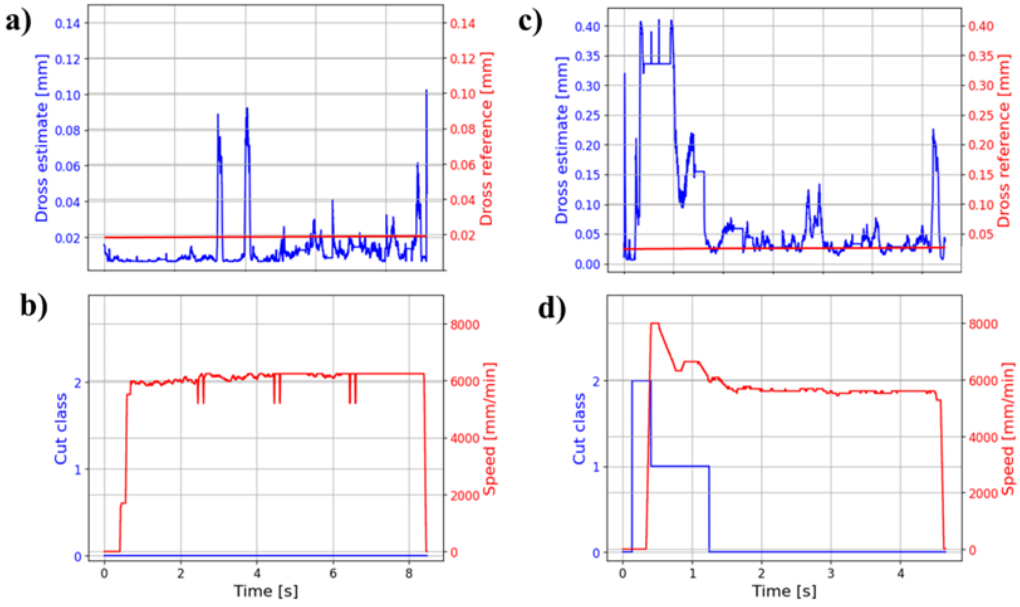

Fig 6. Real-time control experiments realized from different starting conditions (a),(b) standard cut with starting cutting speed of 5200 mm/min and dross reference (red) of 0.02 mm; (c),(d) loss of cut with starting cutting speed of 8000 mm/min and dross reference (red) of 0.02 mm

In both the presented cases, the novel control architecture based on the dross estimate and cut class classifier is capable of correctly detect the process state condition and consequently regulating the cutting speed to the optimal value that guarantees the feasibility of the cut (cut class = 0) and at the same time maximizes productivity and quality by reaching the set dross reference with the highest possible cutting speed value.

Moreover, the productivity increases with respect to the reference speed v_{ref} = 5200 mm/min results in a final cutting speed of 6000 mm/min, enabling an increase of approximately 15%.

3.3 Testing on industrial demonstrator case-study

This section illustrates the final outcome of the demonstrator case study previously introduced in Section 2.5. More in particular, Fig 7(a) illustrates the laser cutting system during the cutting operation, whilst Fig 7(b) shows the final vase demonstrator. Moreover, Fig 7(c) presents the real-time speed regulation during the cutting of a curved line of the vase geometry, highlighted in red in Fig 7(d).

Furthermore, to demonstrate the productivity increase with respect to a standard nominal condition, the same vase geometry was cut on 5 mm thick stainless steel without the real-time speed control, employing the same process parameters of Section 2.5 and a standard cutting speed of 5200 mm/min.

It's important to underline that during the vase demonstrator case, the real-time control architecture guarantees an overall cutting time decrease of approximately 30 s enabling a productivity increase of around 15%, according to the previous realized control experiments.

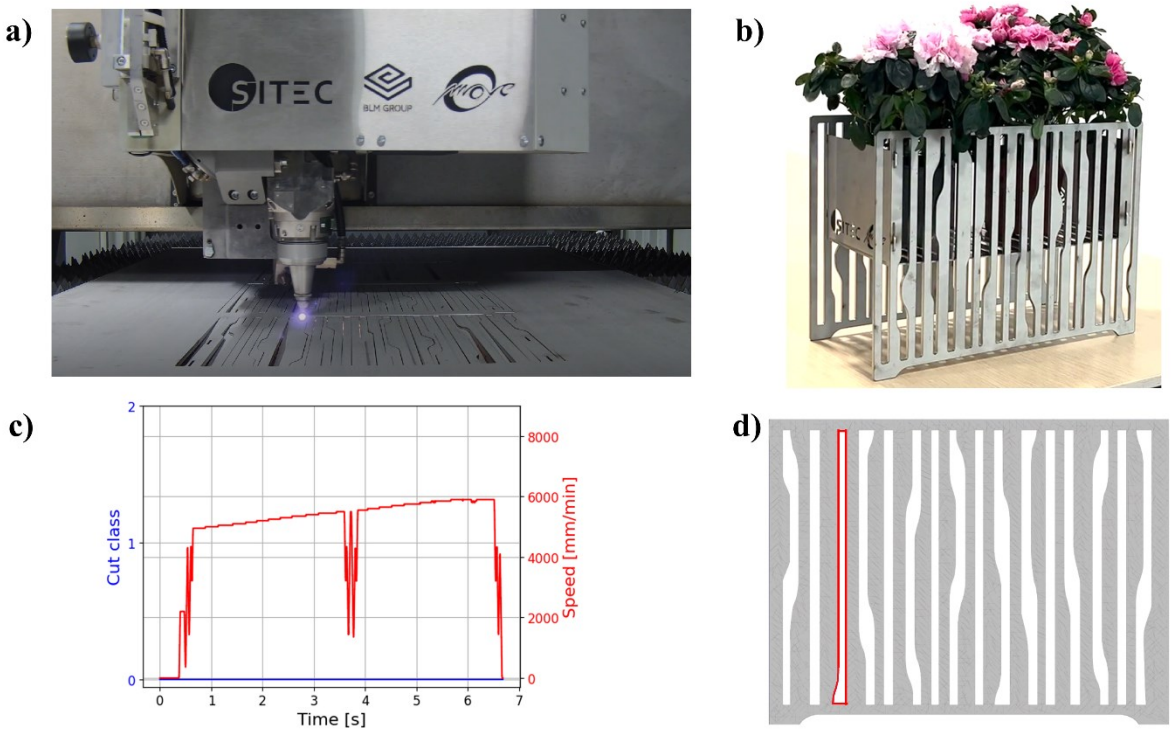

Fig. 7. (a) Laser cutting system during the cutting phase of the vase demonstrator case; (b) final vase demonstrator; (c) real-time speed control regulation during a curved line of the vase geometry, as represented and highlighted in red in (d)

4. Conclusions

The present work develops a control approach to regulate in real time the cutting speed of stainless steel fiber laser cutting process. A coaxial camera monitoring architecture was employed to extract process relevant information and correlate them to the observed cut quality, in terms of both dross attachment and process state. The main results can be summarized as follows:

- A supervised cut class classifier was developed to detect in real time the process state from the collected camera frames with an overall accuracy of the model above 99%.
- The mentioned cut class classifier was integrated with a NN dross estimate model into a closed-loop control architecture, tested with real-time control experiments.
- The presented approach was finally tested on a complex geometry case study, demonstrating the system feasibility and capabilities on relevant industrial scenarios whilst guaranteeing the reduction of the cutting time and an increase of the process productivity of approximately 15%.

Acknowledgments

The credit for the concept, design, and engineering of the demonstrator is attributed to Valentine Lechien. The authors also sincerely thank Valentine for the excellent work carried out, as well as for the support and assistance provided in the development of this research.

Moreover, the Italian Ministry of Education, University and Research is acknowledged for the support provided through National Plan of Recovery and Resilience (PNRR).

References

Adelmann, B., Schleier, M., Neumeier, B., & Hellmann, R. (2016). Photodiode-based cutting interruption sensor for near-infrared lasers. *Applied Optics*, *55*(7), 1772. https://doi.org/10.1364/ao.55.001772

Guerra, S., Caprio, L., Pacher, M., Gandolfi, D., Previtali, B., Savaresi, S. M., & Tanelli, M. (2024). *Real-time grid detection in sheet metal fiber laser cutting through coaxial monitoring* (13th CIRP Conference on Photonic Technologies [LANE 2024], Ed.; pp. 15–19). www.sciencedirect.comwww.elsevier.com/locate/procedia2212-8271

Guerra, S., Vazzola, L., Caprio, L., Pacher, M., Gandolfi, D., Tanelli, M., Savaresi, S. M., & Previtali, B. (2025). Velocity-based closed-loop control in fusion laser cutting for multi-directional and curved geometries. *Journal of Laser Applications*, *37*(1). https://doi.org/10.2351/7.0001617

Mazzoleni, L., Demir, A. G., Caprio, L., Pacher, M., & Previtali, B. (2020). Real-Time Observation of Melt Pool in Selective Laser Melting: Spatial, Temporal, and Wavelength Resolution Criteria. *IEEE Transactions on Instrumentation and Measurement*, *69*(4), 1179–1190. https://doi.org/10.1109/TIM.2019.2912236

Pacher, M., Franceschetti, L., Strada, S. C., Tanelli, M., Savaresi, S. M., & Previtali, B. (2020). Real-time continuous estimation of dross attachment in the laser cutting process based on process emission images. *Journal of Laser Applications*, *32*(4), 042016. https://doi.org/10.2351/7.0000145

Pacher, M., Gandolfi, D., Tanelli, M., Previtali, B., Savaresi, S., Finazzi, V., Piccoli, F., & Delama, G. (n.d.-a). *Procedimento e macchina per una lavorazione laser*.

Pacher, M., Gandolfi, D., Tanelli, M., Previtali, B., Savaresi, S. M., Finazzi, V., Piccoli, F., & Delama, G. (n.d.-b). *Method of and machine for a laser processing with roughness estimation*.

Pacher, M., Mazzoleni, L., Caprio, L., Demir, A. G., & Previtali, B. (2019). Estimation of melt pool size by complementary use of external illumination and process emission in coaxial monitoring of selective laser melting. *Journal of Laser Applications*, *31*(2). https://doi.org/10.2351/1.5096117

Pacher, M., Strada, S., Tanelli, M., Previtali, B., Savaresi, S. M., & Spa, A. (n.d.). *Real-time velocity regulation for productivity optimization in laser cutting*.

Poprawel, R., & Konig, W. (2001). Modeling, Monitoring and Control in High Quality Laser Cutting. *CIRP Annals*, *50*(1), 137–140.

Schleier, M., Adelmann, B., Neumeier, B., & Hellmann, R. (2017). Burr formation detector for fiber laser cutting based on a photodiode sensor system. *Optics and Laser Technology*, *96*, 13–17. https://doi.org/10.1016/j.optlastec.2017.04.027

Wen, P., Zhang, Y., & Chen, W. (2012). Quality detection and control during laser cutting progress with coaxial visual monitoring. *Journal of Laser Applications*, *24*(3), 032006. https://doi.org/10.2351/1.4719933